A stochastic approach to estimate the uncertainty of dose mapping caused by uncertainties in b-spline registration

Martina Hub[a)]
Department of Medical Physics in Radiation Oncology, German Cancer Research Center (DKFZ), 69120 Heidelberg, Germany

Christian Thieke
Clinical Cooperation Unit Radiation Oncology, German Cancer Research Center (DKFZ), 69120 Heidelberg, Germany and Department of Radiation Oncology, University Clinic Heidelberg, 69120 Heidelberg, Germany

Marc L. Kessler
Department of Radiation Oncology, University of Michigan, Ann Arbor, Michigan 48109

Christian P. Karger
Department of Medical Physics in Radiation Oncology, German Cancer Research Center (DKFZ), 69120 Heidelberg, Germany

(Received 8 November 2011; revised 20 February 2012; accepted for publication 5 March 2012; published 29 March 2012)

Purpose: In fractionated radiation therapy, image guidance with daily tomographic imaging becomes more and more clinical routine. In principle, this allows for daily computation of the delivered dose and for accumulation of these daily dose distributions to determine the actually delivered total dose to the patient. However, uncertainties in the mapping of the images can translate into errors of the accumulated total dose, depending on the dose gradient. In this work, an approach to estimate the uncertainty of mapping between medical images is proposed that identifies areas bearing a significant risk of inaccurate dose accumulation.
Methods: This method accounts for the geometric uncertainty of image registration and the heterogeneity of the dose distribution, which is to be mapped. Its performance is demonstrated in context of dose mapping based on b-spline registration. It is based on evaluation of the sensitivity of dose mapping to variations of the b-spline coefficients combined with evaluation of the sensitivity of the registration metric with respect to the variations of the coefficients. It was evaluated based on patient data that was deformed based on a breathing model, where the ground truth of the deformation, and hence the actual true dose mapping error, is known.
Results: The proposed approach has the potential to distinguish areas of the image where dose mapping is likely to be accurate from other areas of the same image, where a larger uncertainty must be expected.
Conclusions: An approach to identify areas where dose mapping is likely to be inaccurate was developed and implemented. This method was tested for dose mapping, but it may be applied in context of other mapping tasks as well. © *2012 American Association of Physicists in Medicine*. [http://dx.doi.org/10.1118/1.3697524]

Key words: fractionated radiation therapy, dose accumulation, dose mapping, b-spline registration, accuracy, uncertainty

I. INTRODUCTION

The transfer of any spatially distributed quantity from one coordinate system to another can be called mapping and requires knowledge of the underlying geometric transformation between both coordinate systems. One possible application is the mapping of dose between computed tomography (CT) images that are acquired before each treatment in fractioned radiation therapy. Dose distributions may be calculated based on these different CT images, and the process of mapping all the distributions to one CT image and of summing up over the contributions of the different fractions to each voxel of this image is called "dose accumulation."

Mapping of dose between medical images has been applied in research on image guided radiation therapy (IGRT) in context of dose accumulation in the past,[1] and there is a strong need to minimize and characterize the uncertainty of dose accumulation.[2] Since mapping requires knowledge of the geometric transformation between the coordinate systems of images, correct estimation of this transformation is essential, and in case, if it is obtained by image registration, uncertainties of image registration affect the accuracy of dose accumulation, especially in those areas with steep dose gradients, i.e., where the distribution is heterogeneous.

The uncertainty of image registration has extensively been discussed.[3–21] However, more work needs to be done to investigate its influence on the dose mapping uncertainty, which does not only depend on geometric uncertainties but also depend on properties of the dose distribution such as dose gradients. The approach proposed here accounts for both issues.

Recently, a new method was introduced to estimate the dose mapping uncertainty based on the consistency of transformations, resulting from multiple consecutive registrations in reverse directions.[22] It has successfully been applied with a thin plate spline algorithm and different patient data. However, parameterized deformable registration algorithms, such as b-spline registration, are likely to create smooth and invertible deformation fields provided that the number of degrees of freedom is not chosen too high. In this case, registration errors may be obtained in a very consistent way. So, the transformation may be incorrect—and still the algorithm may persistently end up with the same incorrect result. So, the approach proposed in Ref. 22 does not yet account for all sources of uncertainty.

Dose mapping uncertainties in context of nonparameterized image registration have been discussed in Ref. 23. This approach has successfully been applied in context of the demons algorithm and can be applied on other registration methods as well. However, it may not perform well with parameterized methods, such as b-spline registration, since it is based on evaluation of the physical fidelity of the deformation field. Compared to nonparameterized image registration algorithms, b-spline registration is smooth by nature and so it is more likely to run into problems with a potential model mismatch than into problems with the physical fidelity of the deformation field in case the number of knots is not chosen too high. So, this means that the correct deformation (ground truth) may be a deformation that cannot be described by the b-spline model that is applied, in case the number of b-spline knots is chosen too low. Only a very high number of knots may lead to problems with the physical fidelity of the deformation field while a potential model mismatch becomes less likely. Another source of error that is more likely to affect parameterized registration than problems with the physical fidelity of the deformation field is missing structure within the images. This means that, in case, if intensity gradients are missing in some region of the image, then information is missing, which would be needed to guide the deformation process and thus the registration accuracy becomes low. Therefore, an approach to estimate its uncertainty must account for model mismatch and missing structure. These issues are likely to affect parameterized registration methods and need to be taken into account when uncertainty of mapping is estimated rather than problems with the physical fidelity. Therefore, an approach to estimate the dose mapping uncertainty that is tailored toward parameterized image registration is needed and proposed in this work.

In a previous paper, we proposed a stochastic approach to estimate the uncertainty of b-spline image registration.[24] Here, we suggest an extension of this method to address the uncertainty of dose mapping.

II. METHODS AND MATERIALS

II.A. Dose mapping and its dependence on image registration

Dose mapping requires knowledge of the geometric correspondence between the coordinate systems of both images. Image registration is the process of determining the geometric correspondence between these systems, and thus it can supply a dose mapping algorithm with the required information, for example, represented as a displacement vector field (DVF) resulting from b-spline deformable registration.

II.B. B-spline registration and its geometric uncertainty

In b-spline registration, the DVF is represented as a superposition of weighted b-spline basis functions. The weights are called coefficients and are obtained by optimizing a similarity measure. See Refs. 5 and 24 for details. In Ref. 24, we have shown that the local sensitivity of the similarity measure to variations of the b-spline coefficients can be regarded as a measure of registration uncertainty in b-spline registration. Major sources of uncertainty in b-spline registration are missing image structure and thus homogeneous regions, imperfect optimization as well as a potential mismatch of the b-spline model.[24] Obviously, any mapping between medical images based on registration may be affected by these uncertainties.

II.C. Uncertainties in b-spline based dose mapping

In this section, two main sources of error in mapping of medical images are considered.

II.C.1. Fundamental anatomical changes

Since anatomy may change over time, images acquired at different times may reflect these changes. In case tissue is not conserved, registration, and thus mapping, is an ill posed problem, since it is generally impossible to correctly map dose that was applied to tissue that is present in only one of the images. The uncertainty due to this issue can probably not be estimated by any algorithm, and the method proposed here does not aim to solve this problem but should be applied in a context where tissue is preserved.

II.C.2. Uncertainties in image registration

The second major source of error is the geometric uncertainty of the image registration. It affects dose mapping if the mapped distribution is not homogeneous, which is generally the case. The dose mapping uncertainty $\Delta_D(x,y,z)$ is given by:

$$\Delta_D(x,y,z) = \overrightarrow{grad}_D(x,y,z) \cdot \overrightarrow{Reg}_{err}(x,y,z),$$

where $\overrightarrow{grad}_D(x,y,z)$ is the gradient of the dose distribution and $\mathrm{Reg}_{\mathrm{err}}(\mathrm{x},\mathrm{y},\mathrm{z})$ is the error of the image registration.

So, any approach that aims to estimate dose mapping uncertainties needs to account for both: the spatial gradient of the distribution as well as an estimate of the registration uncertainty.

II.D. The proposed algorithm to estimate dose mapping uncertainty

II.D.1. Concept

II.D.1.a. Estimating registration uncertainty. In our previous paper, an algorithm to estimate the uncertainty of

parameterized image registration was proposed.[24] As it is essential for this work, we briefly summarize the results here. The registration algorithm that was applied in this and the previous study is driven by the decent gradient of the sum-of-square-differences (SSD) metric. If the result of the registration was nonambiguous and did represent the underlying deformation correctly, globally, as well as locally, the SSD should increase with any modification of the resulting deformation.

The approach presented here is motivated by considerations about the consequence of adding a small additional random deformation to the deformation that resulted from the b-spline registration. In this context, one might regard a small subpart of the image and evaluate the change of the SSD in this local area. The local SSD is the SSD calculated from this small area, as opposed to the global SSD, which is calculated from the whole image.

There are three possibilities how the local SSD can be affected by the additional random deformation, which was added to the result of the b-spline registration:

1. The local SSD may increase. This is the case if the image does contain sufficient structure in this local area and if this structure reached alignment during the process of image registration. In that case, any additional deformation increases the SSD. In this situation, the alignment is likely to be correct. So, this does not indicate the presence of uncertainty within the regarded subpart of the image, rather the registration is likely to be correct in this specific area.
2. The local SSD may stay unchanged or does not change significantly. This is the case if there is no structure in the local subregion of the image, i.e., if there is a homogeneous brightness within the regarded area. However, structural information is needed to guide the deformation process; so, this indicates uncertainty of the local result.
3. The local SSD may decrease. This is the case if the registration was imperfect within the considered subpart of the image. One reason may be imperfect optimization. In that case, the algorithm has not resulted in a deformation that represents the global minimum of the metric. Another reason may be a mismatch of the b-spline model. In that case the algorithm may have ended up in the global minimum of the SSD metric, but with the given spline model it is impossible to correctly describe the deformation. Please note, that in this case the local decrease of the SSD metric must be accompanied by a global increase. So the local improvement means a deterioration of the global alignment of the whole image. However, since here we are regarding a local sub-section of the image, a local decrease of the SSD may be possible in case of a model miss match.

So, in any position where an additional random deformation does not increase the local SSD, it is not possible to distinguish whether the modified or the initial deformation field is the better estimate. We do not assume that the deformation with the lower local SSD is the better estimate, but it is just impossible to distinguish which one is better. This indicates the presence of uncertainty.

So, the basic idea of this approach is to calculate the local SSD from a small area around each voxel after registration (initial local SSD). The change of the local SSD by randomly performed modifications of the deformation field is monitored for each of these small areas surrounding each voxel. The spatial deviation between the deformation that resulted from the registration (initial deformation) and each of the randomly modified deformations (modified deformations) is calculated in each voxel for different random modifications of the deformation. The largest spatial deviation that was found for any of those modified deformations, which turned out not to increase the local SSD in the regarded local area, is stored. This spatial deviation is the quantity that we regard as a local measure of uncertainty of image registration.[24] Note that solely the local SSD is regarded here, which is calculated from a small environment of each voxel (see Sec. II D 2 for details).

II.D.1.b. Concept of the enhancement to address dose mapping. To estimate the uncertainty of dose mapping, the approach as in Sec. II D 1 a can be extended. The deformation that resulted from the b-spline registration is randomly modified, and for each random modification, the local SSD is recalculated and compared to the initial local SSD. Again, solely, those modified deformations that do not increase the local SSD are further regarded. The modification to address dose mapping is that, among those modified deformations, which do not increase the local SSD, the largest deviation of the mapped dose from the dose mapped to the same location by the initial deformation is determined (please note that the actual spatial deviation between the initial deformation and the modified deformation is not relevant here). The maximum deviation of the mapped dose that was found among those random modifications that did not increase the local SSD is stored as a measure of uncertainty for dose mapping. We call it $\text{Dose}_{\max}$ since it is the maximum deviation of the mapped dose that resulted from any of all the applied random deformations, which did not increase the SSD. Since the deformation corresponding to $\text{Dose}_{\max}$ is not associated with a higher local SSD than the initial result of the registration, it is not possible to tell which deformation is the better local estimate, the recent deformation or the initial deformation. Therefore, the recent dose, mapped to the respective location by the recent modification of the deformation is as likely the correct mapping as the dose that gets mapped to this location by the initial result of the b-spline registration. So, a large deviation between both indicates a large uncertainty.

Note that only the magnitude of the deviation of the dose is regarded; so, $\text{Dose}_{\max}$ is always positive, and we do not distinguish whether the corresponding additional random deformation increases or decreases the dose that gets mapped to the respective voxel. The reason is that the maximum positive deviation may be of similar magnitude as compared to the maximum negative deviation found at a specific voxel. As $\text{Dose}_{\max}$ describes only the potential presence of dose mapping errors rather than the true actual dose mapping error, the sign does not provide any additional relevant information for the clinician.

Section II D 2 describes the algorithm to calculate this measure of uncertainty iteratively.

II.D.2. The algorithm to estimate the local uncertainty

II.D.2.a. First step: initial registration. In this study, the "test image" is a CT image, which is supposed to be warped to match another CT image, which is called "reference image." A dose distribution is associated with this test image and warped, too. The initial deformation field that is needed for this process is obtained by b-spline registration. After b-spline registration, the test image and the dose distribution are mapped to the reference image based on the transformation that was obtained. After this process, the warped dose and the intensity of the warped test image are known in each voxel of the reference image. The local SSD metric is then calculated from a small volume of $3 \times 3 \times 3$ voxels around each voxel, and this value is stored for each voxel as the "initial local SSD."

II.D.2.b. Second step: variation. The variation algorithm proposed here aims to calculate a local measure of uncertainty for each voxel, which we call $\text{Dose}_{\max}$. It is calculated iteratively and set to zero for each voxel at the beginning.

In the first iteration, each coefficient is modified by adding a random number between -9 and $+9$ mm, since registration errors are likely to have a magnitude below 1 cm, while on average, the registration errors are smaller as shown in Refs. 16 and 17. The random numbers are equally distributed. After this modification, the displacement vector field is recalculated and the test image is redeformed. Then, the local metric is recalculated for each voxel from the same small environment, like in step one, and the difference between the actual and the initial local metric is calculated. The dose distribution is redeformed as well, and the magnitude of the difference between the recently and the initially mapped dose is calculated for the centre of each voxel. In case the recent local SSD is smaller than or equal to the initial one, the magnitude of the difference between the actual and the initially mapped dose is stored for each voxel. In case the local metric has increased, $\text{Dose}_{\max}$ remains unchanged.

This variation of the b-spline coefficients is then repeated 400 times, and in each iteration, $\text{Dose}_{\max}$ is replaced only if the local SSD is smaller than or equal to the initial one that was calculated right after the registration and if, at the same time, the replacement leads to storage of a value of $\text{Dose}_{\max}$ that is increased with respect to the previous one. After 400 iterations, $\text{Dose}_{\max}$ represents the largest deviation from the initially mapped dose that was found for any of those random modifications that did not increase the local SSD. This value is regarded as a local measure of the dose mapping uncertainty.

In our setting, the algorithm ran about 15 min on a laptop with a 1.86 GHz single core processor and 32 bit architecture. However, the speed can be improved by an order of magnitude by using modern state-of-the-art computers and parallel processing.

II.E. Evaluation of the proposed algorithm

Validation of the proposed algorithm faces two problems: First, one of the sources of error that we are taking into account is the lack of image structure, and we wanted to evaluate the uncertainty of dose mapping in both, regions with as well as without image structure. In regions without image structure, however, anatomical landmarks are obviously not available, since landmarks can only be represented by image structure. A second problem is that our method is a stochastic approach. So, a large number of control points are necessary, but the number of landmarks that can be picket precisely is very limited, especially in those areas where image structure is missing. So, picking landmarks is not feasible to validate the algorithm. To circumvent these problems, a test data set was created based on a deformation model. Here, the ground truth of the deformation and hence the true deformation and dose mapping errors are known, and so this data set was used to test the proposed method as described below.

II.E.1. Test data

The proposed method was tested using a single CT image of the thorax of a patient, an exhale image of a 4D CT. An additional CT image, representing an inhale image, was generated by artificially deforming the exhale image. Therefore, the ground truth on the deformation and the true dose mapping errors are known and can be compared with the uncertainty estimation by the proposed algorithm.

The deformation model has been described previously in detail,[24] and so only the main features are described here. The deformation model contains the following aspects of respiratory motion:

II.E.1.a. Expansion of the lung in craniocaudal direction during inhale. This aspect was modeled by an offset to the craniocaudal component of the displacement vectors. The offset is constant throughout each transversal plane and decreases in cranial direction. In the area below the diaphragm, the offset is set constant for all voxels. The magnitude of the decompression ranged between 25 mm at the diaphragm and 0 mm at the top of the lung.

II.E.1.b. Dilation of the chest wall in the transversal plane. Dilation was simulated by scaling the chest wall in the transversal plane. So, a point in the center of the patient and in the region of the diaphragm was chosen, and a deformation field was then created to stretch the rib cage in each transversal plane as a function of the distance from this point. The scaling factor decreases in caudal direction and is constant below the diaphragm.

II.E.1.c. Tissue sliding between the lung and the rib cage. To describe tissue sliding between the lung and the rib cage, a segmentation of the rib cage was performed. The sliding was then modeled based on two different deformation fields to describe the deformation inside and outside the rib cage. The displacement vector field to describe the deformation inside the lung is a superposition of the deformation fields resulting from step one and two as described above (denoted as $\text{DVF}_{\text{internal}}$). The deformation field to describe the deformation outside the lung ($\text{DVF}_{\text{external}}$) is obtained from $\text{DVF}_{\text{internal}}$ by setting the craniocaudal component of $\text{DVF}_{\text{internal}}$ to zero. $\text{DVF}_{\text{external}}$ is then modified such that the

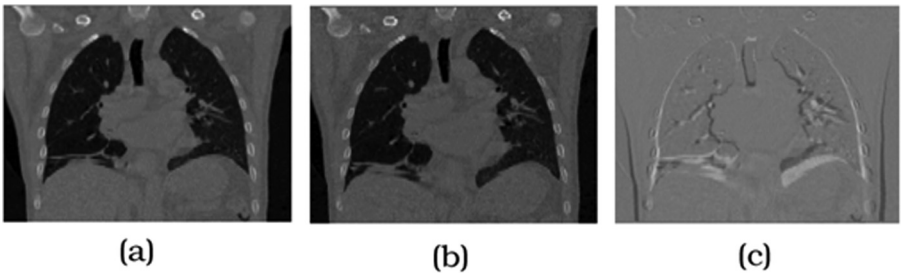

FIG. 1. (a) Exhale image taken from the 4DCT image set; (b) simulated inhale; and (c) difference image between exhale and simulated inhale image.

boundary region between inside and outside the rib cage is mapped to the same surface by both deformation fields. As described in Ref. 24, this is done with the help of an image registration of two masked images of the lung that were deformed based on the two different deformation fields $DVF_{internal}$ and $DVF_{external}$.

The combined deformation field of the steps one to three is then given by $DVF_{internal}$ for the region inside and $DVF_{external}$ for the region outside the rib cage. The 4DCT exhale image is then warped with this combined deformation field to obtain the simulated inhale image.

Figure 1 shows the simulated inhale image, which was used as reference image as well as the exhale image that was taken from the 4DCT image set and the difference image between the simulated inhale and the exhale image of the 4DCT.

II.E.2. Evaluation

After applying the proposed algorithm on the test data, $Dose_{max}$ is know in each voxel. For our test data set, the ground truth of the deformation, and hence the true dose mapping error, is known as well. Therefore, it is possible to show the relationship between estimated and true dose mapping error. For this purpose, the voxels are binned according to the magnitude of $Dose_{max}$, and the average local dose mapping error (ground truth) is then calculated for the respective bin. The average local dose mapping error is then plotted against $Dose_{max}$ as a histogram to show the dependency between average $Dose_{max}$ within the respective bin and the local dose mapping error averaged over voxels of this bin and therefore averaged over voxels with similar $Dose_{max}$.

III. RESULTS

Figure 2 displays the dependency between the proposed uncertainty measure $Dose_{max}$ and the true dose mapping error. The histogram in Fig. 2(a) shows that the dose mapping error averaged over each bin clearly increases with increasing $Dose_{max}$. So, for those voxels with a large $Dose_{max}$, a larger dose mapping error can be expected compared to those voxels, where $Dose_{max}$ is small. The bounds of the bins are not equidistant, but chosen such, that the same number of voxels contribute to each bin. The increase of the bin size (distance between left and right border of each bin) strongly increases toward the right hand of Figs. 2(a) and 2(b), which shows that the number of voxels per interval of $Dose_{max}$ decreases with increasing $Dose_{max}$. So, the number of voxels with large values of $Dose_{max}$ is low; however, those voxels that have a large measure of uncertainty, on average, are indeed associated with a large dose mapping error. Figure 2(b) demonstrates that, among voxels with similar $Dose_{max}$, a large variation of the actual registration error can be found. The reason is that, although the image registration error may potentially be large in those areas, where the image registration metric is insensitive to

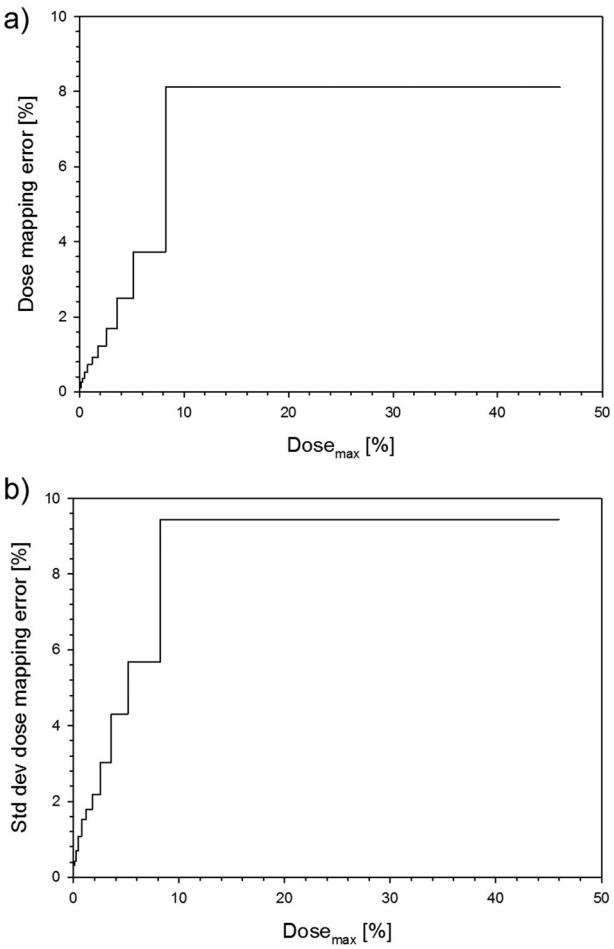

FIG. 2. (a) True dose mapping error as a function of $Dose_{max}$ and (b) Standard deviation of the dose mapping error (ground truth) within each respective bin and thus as a function of $Dose_{max}$. The bin sizes are chosen such that the number of voxels that contribute to each histogram bin is the same. So, the bounds of the bins are not equidistant. Dose mapping error as well as $Dose_{max}$ are denoted in percent of the prescribed dose.

variations of the b-spline coefficients due to missing structure, the result does not necessarily have to be incorrect, since the algorithm may have found the correct displacement in this point by chance although information was missing.

Figure 3 displays a transversal and a coronal CT image slice (a, b) and the respective dose distributions (c, d) as well as the true dose mapping error (e, f), which is known for this specific test case as well as the proposed uncertainty measure Dose_{max} (g, h). Note that the coronal slice does not intersect the tumour, because, in the area of the tumor, the dose is rather homogenous and thus not so interesting since the region where dose mapping errors actually appear is the area with dose gradients, which is displayed here, see (c, d). The images displaying Dose_{max} look similar to those that show the true dose mapping error, which suggests a correlation. The correlation coefficient between both quantities was calculated for the whole dataset, including all voxels, and a value of 0.59 was obtained. So, Dose_{max} or an image displaying this quantity as in Figs. 3(g) and 3(h) can be used to show areas where the dose mapping must be expected to be uncertain.

IV. DISCUSSION

This paper addresses the uncertainty of dose mapping that appears due to geometric uncertainties in image registration. Different approaches have been proposed to estimate the uncertainty of dose mapping. One is based on the consistency of transformations, resulting from multiple consecutive registrations in reverse directions.[22] Dose mapping uncertainties in context of nonparameterized image registration have been discussed in Ref. 23. Although both methods have successfully been applied, they yet do not account for all sources of uncertainty. As opposed to other approaches this one is tailored toward parameterized registration methods, and we demonstrate its performance with b-spline

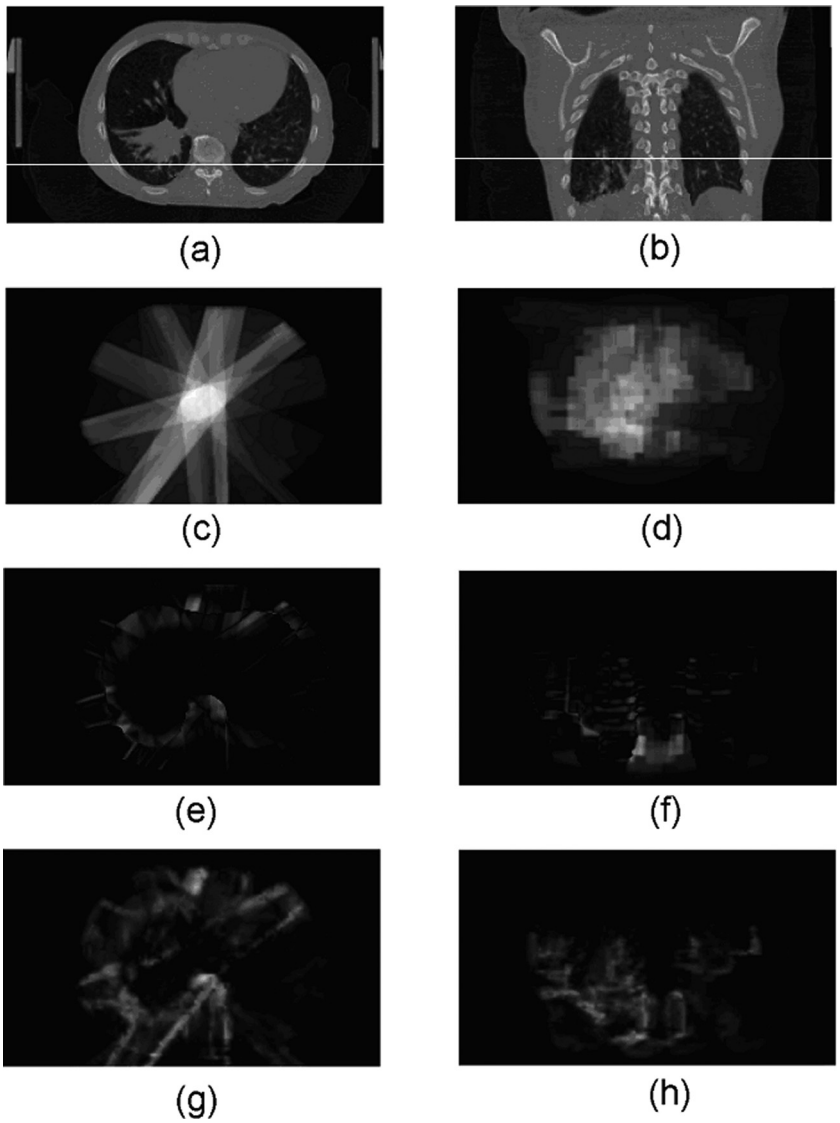

FIG. 3. Topographic display of the dose mapping error and the estimate, black represents zero and white the maximum value that appeared in the image. (a) Transversal CT image slice, the white line in (b) shows the location of this transversal slice in the coronal view; (b) Coronal CT image slice, the white line in (a) shows the location of this coronal slice in the transversal view (c, d) dose distribution of the same slice as in (a, b); (e, f) the true dose mapping error, which is known for this test case where the ground truth of the deformation is known; and (g, h) estimate of Dose_{max}.

registration. It accounts for problems due to homogeneity as well as misalignment of image structure after registration. However, it does not aim to solve the mapping problem in context of tissue growth or shrinkage, since this is an ill posed mapping problem, because it is generally incorrect to map dose that was applied to tissue that is present in just one of the images. So, this method can be applied in a context or in a subpart of an image, where tissue growth or shrinkage is not significant. This restriction, however, is not specific to this approach, rather this is likely to hold for any algorithm to estimate dose mapping uncertainties.

This method does not aim to determine the true dose mapping error; rather, $\text{Dose}_{\max}$ provides information, whether a large dose mapping error must be expected in a specific image region, compared to other areas of the same image. The correlation coefficient that expresses the relation between the true dose mapping error and the proposed quantity as well as the curve in Fig. 3 show that $\text{Dose}_{\max}$ can successfully discriminate such regions.

When it comes to clinical application of dose mapping, tools will be needed, which remind physicians of the dose mapping uncertainty and, moreover, which identify those image regions where these uncertainties are likely to be a problem. The display of $\text{Dose}_{\max}$ images as in Fig. 3 may be helpful for this. In this context, in regions with high values of $\text{Dose}_{\max}$, small dose mapping errors are possible, but, in areas with small $\text{Dose}_{\max}$, large dose mapping errors are not likely to appear (Fig. 2).

V. CONCLUSION

An approach to identify areas where dose mapping is likely to be inaccurate was developed and implemented. It was evaluated based on artificially created test data and has the potential to distinguish areas of the image where dose mapping is uncertain from areas of the same image where large dose mapping errors are unlikely. This method was tested for dose mapping, but it may be applied in context of other mapping tasks as well.

ACKNOWLEDGMENT

Parts of this work were supported by the German Federal Ministry of Education and Research (Grant No. 01IB08002 "DOT-MOBI").

[a]Author to whom correspondence should be addressed. Electronic mail: m.hub@dkfz.de

[1]M.Rosu, J. M. Balter, I. J. Chetty, M. L. Kessler, D. L McShan, P. Balter, and R. K. Ten Haken, "How extensive of a 4D dataset is needed to estimate cumulative dose distribution plan evaluation metrics in conformal lung therapy?," Med. Phys. **34**(1), 233–245 (2007).

[2]D. A. Jaffray, P. E. Lindsay, K. K. Brock, J. O. Deasy, and W. A. Tome, "Accurate accumulation of dose for improved understanding of radiation effects in normal tissue," Int. J. Radiat. Oncol., Biol., Phys. **76**(3), 135–139 (2010).

[3]M. L. Kessler, "Image registration and data fusion in radiation oncology," Br. J. Radiol. **79**, 99–108 (2006).

[4]H. Wang, L. Dong, J. O'Daniel, R. Mohan, A. S. Garden, K. K. Ang, D. A. Kuban, M. Bonnen, J. Y. Chang, and R. Cheung, "Validation of an accelerated 'Demons' algorithm for deformable image registration in radiation therapy," Phys. Med. Biol. **50**, 2887–2905 (2005).

[5]J. Kybic and M. Unser, "Fast parametric elastic image registration," IEEE Trans. Image Process. **12**, 1427–1442 (2003).

[6]J. Kybic, "Image registration accuracy evaluation without ground truth," Proceedngs of IEEE ISBI 2008, May 2008, Paris.

[7]K. K. Brock, M. B. Sharp, L. A. Dawson, S. M. Kim, and D. A. Jaffray, "Accuracy of finite element model-based multi-organ deformable image registration," Med. Phys. **32**, 1647–1659 (2005).

[8]M. M. Coselmon, J. M. Balter, D. L. McShan, and M. L. Kessler, "Mutual information based CT registration of the lung at exhale and inhale breathing states using thin-plate splines," Med. Phys. **31**, 2942–2948 (2004).

[9]E. Rietzel and G. T. Y. Chen, "Deformable registration of 4D computed tomography data," Med. Phys. **33**, 4423–4430 (2006).

[10]E. Heath, D. L. Collins, P. J. Keall, L. Dong, and J. Seuntjens, "Quantification of accuracy of the automated nonlinear image matching and anatomical labeling (ANIMAL) nonlinear registration algorithm for 4D CT images of lung," Med. Phys. **34**(11), 4409–4421 (2007).

[11]K. Wijesooriya, E. Weiss, V. Dill, S. Joshi, and P. J. Keall, "Quantifying the accuracy of automated structure segmentation in 4D CT images using a deformable image registration algorithm," Med. Phys. **35**(4), 1251–1260 (2008).

[12]J. A. Schnabel, C. Tanner, A. D. Castellano-Smith, A. Degenhard, M. O. Leach, D. R. Hose, and D. L. G. Hill, "Validation of nonrigid image registration using finite-element methods: Application to breast MR images," IEEE Trans. Med. Imaging **22**, 238–247 (2003).

[13]P. Rogelj and S. Kovacic, "Symmetric image registration," Med. Image Anal. **10**(3), 484–493 (2006).

[14]J. D. Lawson, E. Schreibmann, A. B. Jani, and T. Fox, "Quantitative evaluation of a cone-beam computed tomography-planning computed tomography deformable image registration method for adaptive radiation therapy," J. Appl. Clin. Med. Phys. **8**(4), 2432 (2007).

[15]M. Serban, E. Heath, G. Stroian, D. L. Collins, and J. Seuntjens, "A deformable phantom for 4D radiotherapy verification: Design and image registration evaluation," Med Phys. **35**(3), 1094–1102 (2008).

[16]R. Kashani, J. Balter, M. Kessler, M. Hub, L. Dong, L. Zhang, L. Xing, Y. Xie, D. Hawkes, J. Schnabel, J. McClelland, and S. Joshi, "Objective assessment of deformable image registration in radiotherapy—A multi-institution study," 49th AAPM Annual Meeting, Minneapolis, MN, July 22–26 (2007).

[17]R. Kashani, M. Hub, J. M. Balter, M. L. Kessler, L. Dong, L. F. Zhang, L. Xing, Y. Q. Xie, D. Hawkes, J. A. Schnabel, J. McClelland, S. Joshi, Q. Chen, and W. G. Lu "Objective assessment of deformable image registration in radiotherapy—A multi-institution study," Med. Phys. **35**(12), 5944–5953 (2008).

[18]M. Söhn, M. Birkner, Y. Chi, J. Wang, Y. Di, B. Berger, and M. Alber, "Model-independent, multimodality deformable image registration by local matching of anatomical features and minimization of elastic energy," Med. Phys. **35**(3), 866–878 (2008).

[19]J. Kybic, "Bootstrap resampling for image registration uncertainty estimation without ground truth," IEEE Trans. Image Process. **19**(1), 64–73 (2010).

[20]R. Floca and H. Dickhaus, "A flexible registration and evaluation engine (f.r.e.e.)," Comput. Methods Programs Biomed. **87**(2), 81–92 (2007).

[21]H. Prüm, L. Gerigk, C. Hintze, C. Thieke, and R. Floca, "Softwareunterstützte Standardisierung manueller Landmarken in medizinischen Bildern," Z. Med. Phys. **21**(1), 42–51 (2011).

[22]F. J. Salguero, N. K. Saleh-Sayah, C. Y. Yan, and J. V. Siebers, "Estimation of three-dimensional intrinsic dosimetric uncertainties resulting from using deformable image registration for dose mapping," Med. Phys. **38**(1), 343–353 (2011).

[23]H. Zhong, E. Weiss, and J. V. Siebers, "Assessment of dose reconstruction errors in image-guided radiation therapy," Phys. Med. Biol. **53**(3), 719–736 (2008).

[24]M. Hub, M. L. Kessler, and C. P. Karger, "A stochastic approach to estimate the uncertainty involved in B-spline image registration," IEEE Trans. Med. Imaging **28**(11), 1708–1716 (2009).